RSC Advances

PAPER

View Article Online
View Journal | View Issue

Cite this: *RSC Adv.*, 2020, **10**, 7368

It takes two for chronic wounds to heal: dispersing bacterial biofilm and modulating inflammation with dual action plasma coatings†

Thomas Danny Michl, ‡* Dung Thuy Thi Tran,‡ Hannah Frederike Kuckling, Aigerim Zhalgasbaikyzy, Barbora Ivanovská, Laura Elena González García, Rahul Madathiparambil Visalakshan and Krasimir Vasilev

Chronic wounds are affecting increasingly larger portions of the general population and their treatment has essentially remained unchanged for the past century. This lack of progress is due to the complex problem that chronic wounds are simultaneously infected and inflamed. Both aspects need to be addressed together to achieve a better healing outcome. Hence, we hereby demonstrate that the stable nitroxide radical (2,2,6,6-tetramethylpiperidin-1-yl)oxyl (TEMPO) can be plasma polymerized into smooth coatings (TEMPOpp), as seen *via* atomic force microscopy, X-ray photoelectron spectroscopy and ellipsometry. Upon contact with water, these coatings leach nitroxides into aqueous supernatant, as measured *via* EPR. We then exploited the known cell-signalling qualities of TEMPO to change the cellular behaviour of bacteria and human cells that come into contact with the surfaces. Specifically, the TEMPOpp coatings not only suppressed biofilm formation of the opportunistic bacterium *Staphylococcus epidermidis* but also dispersed already formed biofilm in a dose-dependent manner; a crucial aspect in treating chronic wounds that contain bacterial biofilm. Thus the coatings' microbiological efficacy correlated with their thickness and the thickest coating was the most efficient. Furthermore, this dose-dependent effect was mirrored in significant cytokine reduction of activated THP-1 macrophages for the four cytokines TNF-α, IL-1β, IL-6 and IP-10. At the same time, the THP-1 cells retained their ability to adhere and colonize the surfaces, as verified *via* SEM imaging. Thus, summarily, we have exploited the unique qualities of plasma polymerized TEMPO coatings in targeting both infection and inflammation simultaneously; demonstrating a novel alternative to how chronic wounds could be treated in the future.

Received 26th November 2019
Accepted 6th February 2020

DOI: 10.1039/c9ra09875e

rsc.li/rsc-advances

Introduction

Chronic wounds are the classic "chicken or egg" paradox because they are simultaneously infected and inflamed, while it is not known which came first.[1–3] Chronic wounds are categorised as either pressure, diabetic or vascular ulcers that won't heal on their own. Chances are, one knows a person who is affected, as 1–2% of the population suffer from chronic wounds.[4] In hospitals, this prevalence is even higher; reports vary but can be placed between single digits up to 28% among in-house patients.[5]

This high prevalence translates into incalculable suffering, loss of limbs and lives as well as 2–3% of the combined healthcare costs in developed countries.[6] In anticipation of an age-friendly world, we have to anticipate chronic wounds being a significant and growing antagonist. Most research avenues aim to prevent biofilm formation in the first place. However, this is a pointless endeavour for chronic wounds, which already have a pre-formed biofilm that requires dispersal.[7] Medicinal recommendations are advising against the topical use of disinfectants or antibiotics on chronic wounds as they can damage healthy tissue and lead to drug-resistant pathogens.[8] Instead, the current practice is "mechanical" debridement of the chronic wound, as washing with aqueous solutions has proven ineffective.[9] Despite causing severe discomfort to the patient and potentially damaging healthy tissue, mechanical debridement does not break up biofilm on the microscopic level. However, systemic antibiotics are not advised unless sepsis occurs.[8] In essence, most of the medical progress in the past 100 years has not led to substantial improvement in how chronic wounds are treated.

Novel strategies have emerged to break up biofilm on the microscopic level using small molecules that can diffuse through the established biofilm and affect the bacteria's quorum system. The most famous example is nitric oxide which is a key messaging molecule in eukaryotes and prokaryotes

School of Engineering, University of South Australia, Mawson Lakes, Australia. E-mail: thomas.michl@unisa.edu.au

† Electronic supplementary information (ESI) available. See DOI: 10.1039/c9ra09875e

‡ These two authors contributed equally.

alike; having the ability to induce biofilm dispersal and modulate inflammation.[10,11] However, the short half-life of 5 seconds require its constant production and precise dosage limit its usefulness for chronic wound treatment.[12] Alternative approaches that disperse established biofilm involve enzymes, specific peptides and other small molecules such as insulin and bacterial surfactants.[7,13,14] Moreover, aspects such as host-toxicity and bio-degradation are currently unknown and thus may limit these compounds' applicability. Furthermore, these compounds only address one half of the equation for chronic wounds; namely the biofilm dispersion and not the other half, the chronic inflammation.

Thus, effectively breaking the vicious cycle of chronic inflammation and bacterial infection requires a simultaneous two-in-one approach. Nitroxides, such as TEMPO ((2,2,6,6-tetramethylpiperidin-1-yl)oxyl), are stable radicals that have demonstrated to be useful both for biofilm dispersion and for modulating inflammation.[15–23] However, their incorporation into coatings and polymers has proven to be a tedious multi-step endeavour which in turn limits their usefulness, albeit being a currently highly investigated material class.[23,24] In contrast, plasma polymerization is a one-step, rapid and solvent-free process that can be rapidly scaled to industrial-scale.[25–28] Our greater aim is simple: to coat wound dressings with a plasma polymer layer that simultaneously down-regulates inflammation and breaks up established bacterial biofilm. Thus, turning wound dressings from passive "passengers" into pro-active "actors" (Scheme 1).

As a first step, we have recently demonstrated that TEMPO can be successfully plasma polymerized into thin film coatings that prevent biofilm formation.[29] Now, we would like to add another key puzzle piece to our findings by demonstrating that these coatings are also capable of dissolving already formed biofilm by the opportunistic bacteria *Staphylococcus epidermidis* (*S. epidermidis*) that is commonly found in chronic wounds.[30] Furthermore, we would like to show how these coatings modulate the cytokine expression of THP-1 macrophages in a dose-responsive manner. These findings, taken together, are a crucial step towards a new generation of wound dressings that supersede the currently century-old method of how chronic wounds are treated.

Results and discussion

We have previously reported the one-step plasma polymerization of TEMPO and reported its abilities to affect biofilm formation.[29] In this work, we changed the plasma reactor setup and explored how deposition times affect the coatings composition, morphology and stability. We chose silicon wafers, cut into 1 cm × 1 cm squares, due to their ease of use, atomic composition and excellent flatness. All these aspects greatly simplified the characterization of the TEMPOpp coatings and allowed for sharper micrographs. Naturally, silicon is not suitable as a material for wound dressings but because plasma processes are substrate independent,[31] the resulting coatings, in future, can be easily transferred to wound dressings. As can be seen in Fig. 1A, the atomic composition of the TEMPO plasma polymers (TEMPOpp) changes only minutely with different deposition times (5, 15 and 30 min), as expected for plasma polymers, and coincides well with our previous findings which

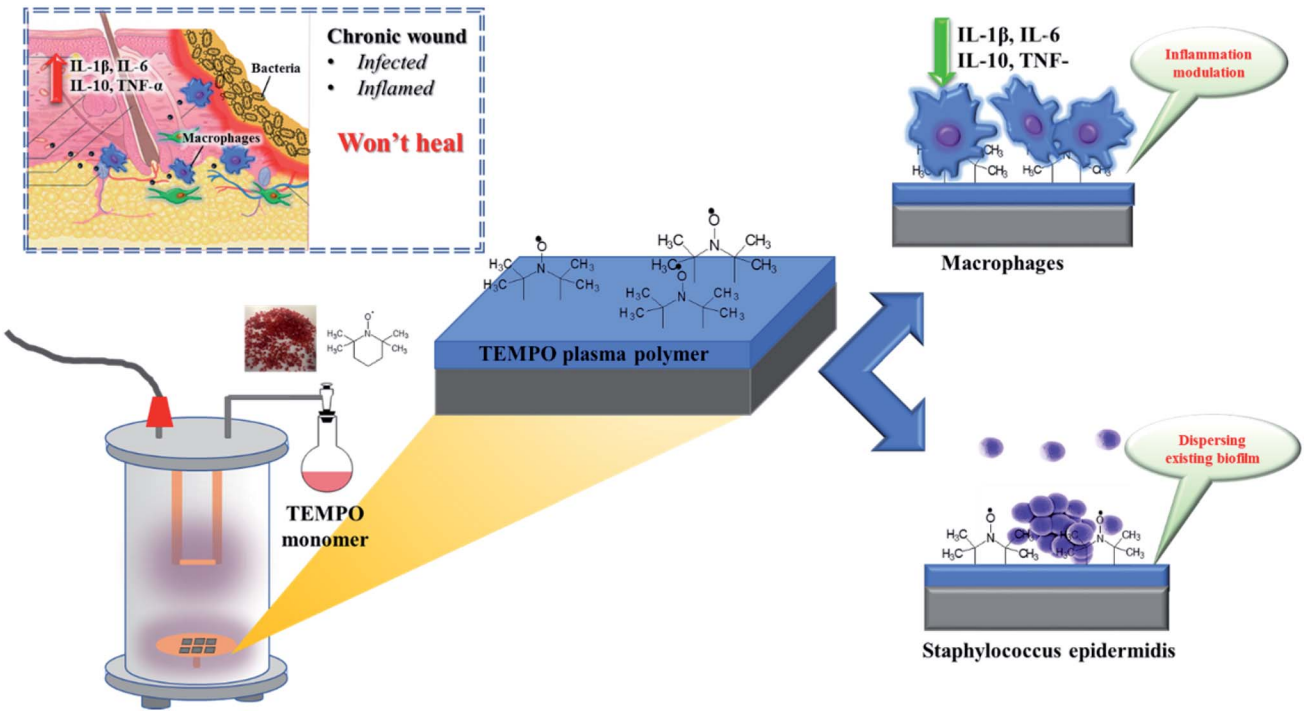

Scheme 1 Chronic wounds are simultaneously infected and inflamed. The stable nitroxide precursors TEMPO was plasma polymerized into thin coatings which were subsequently challenged with the opportunistic bacterium *S. epidermidis* and activated THP-1 macrophages.

A)

	Precursor	%C	%O	%N
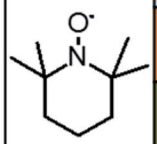	TEMPO	81.8	9.1	9.1
	TEMPOpp 5min	82.1	8.8	9.1
	TEMPOpp 15min	82.6	8.4	9
	TEMPOpp 30min	83.3	7.5	9.2

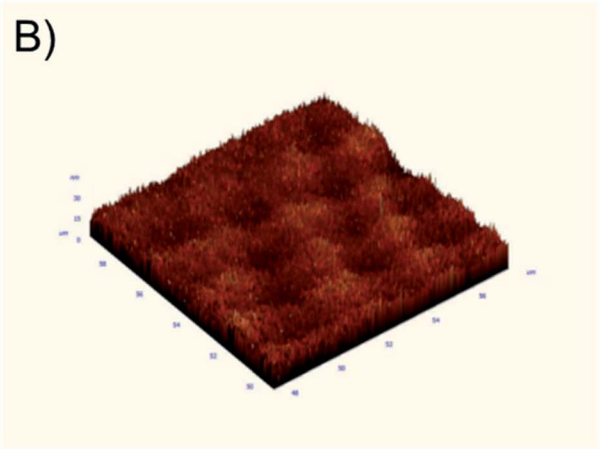

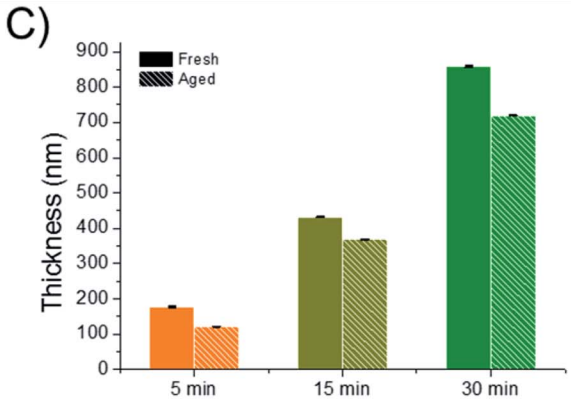

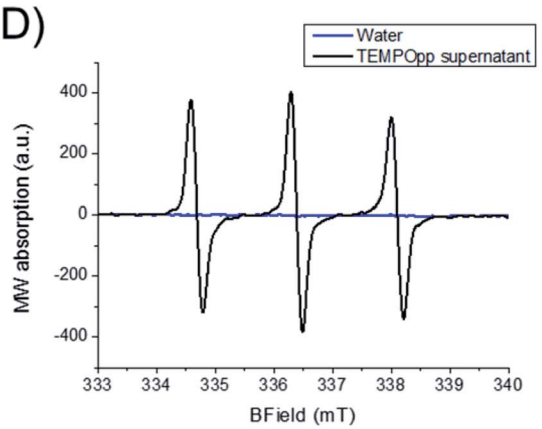

Fig. 1 (A) Atomic percentages of TEMPOpp 5, 15 and 30 min as determined *via* XPS (B) AFM surface image of TEMPOpp 30 min (C) thickness of TEMPOpp 5, 15 and 30 min as determined *via* ellipsometry, error bars represent standard deviation as calculated from the used cauchy model (D) EPR signal of pure water (negative control) and supernatant that was in contact with TEMPOpp 30 min overnight.

were conducted in a different plasma reactor.[29] This finding is interesting because both the nitrogen and oxygen percentage of the monomer are preserved in the resulting coating. For most other nitrogen-containing precursors, such as amines and oxazolines, this does not hold true as during the plasma deposition nitrogen-bearing species are eliminated (reducing the % N) and post plasma oxidation is evident (increasing % O).[28,32–35] This peculiarity of TEMPOpp, which has been observed by us now in two different plasma reactor set-ups, is an ongoing investigation into the deposition mechanism itself, which we will detail separately in a future publication.

Fig. 1B depicts the AFM image of the thickest of the plasma polymers (TEMPOpp 30 min). Additional AFM images of TEMPOpp 5 min & 15 min are depicted in Fig. S1.† As typical for plasma polymers deposited at reduced pressure, the coating is smooth on a nanoscale with a root mean roughness (RMS) of 3.8 nm.[36,37] This may not always be the case as the gas-phase reaction can be rapid and lead to the formation of microscopic "dust-like" particles that embed into the forming coating.[38] These plasma coatings, usually resulting from conditions that are monomer-rich and power-poor, lead to coatings that are heterogeneous in morphology and chemistry. We aimed to exclude the factor of surface topography in the subsequent biological experiments, which has been recently reported upon in-depth.[39,40] Thus, producing homogenous coatings with low RMS eliminated this additional factor in the downstream experiments.

The TEMPOpp thickness was evaluated *via* ellipsometry (Fig. 1C). As anticipated, the thickness correlates with deposition time, as is typical for most plasma polymers;[41–43] this allows for "dialling" in the thickness of the plasma polymer coating at will. Since our previous report on the TEMPOpp coatings, we have been interested in how they exert their biological activity. We suspected that the coatings themselves are not thoroughly cross-linked and thus TEMPO-oligomers can diffuse out into solution which in turn cause the biological effects that we have observed. Thus, we decided to compare the thickness of the coatings after storing them in ambient air for four months. Interestingly, the very same coatings decreased in thickness during that time. This observation hints at the coatings being an intertwined two-component mixture: one component cross-linked, thus involatile, and the other poorly interconnected and inlaid within, making it mobile. Therefore, the mobile component can, over time, evaporate from the coatings and cause a loss of thickness. This loss of thickness was the most pronounced for the thinner coating (TEMPOpp 5 min – 31.4%)

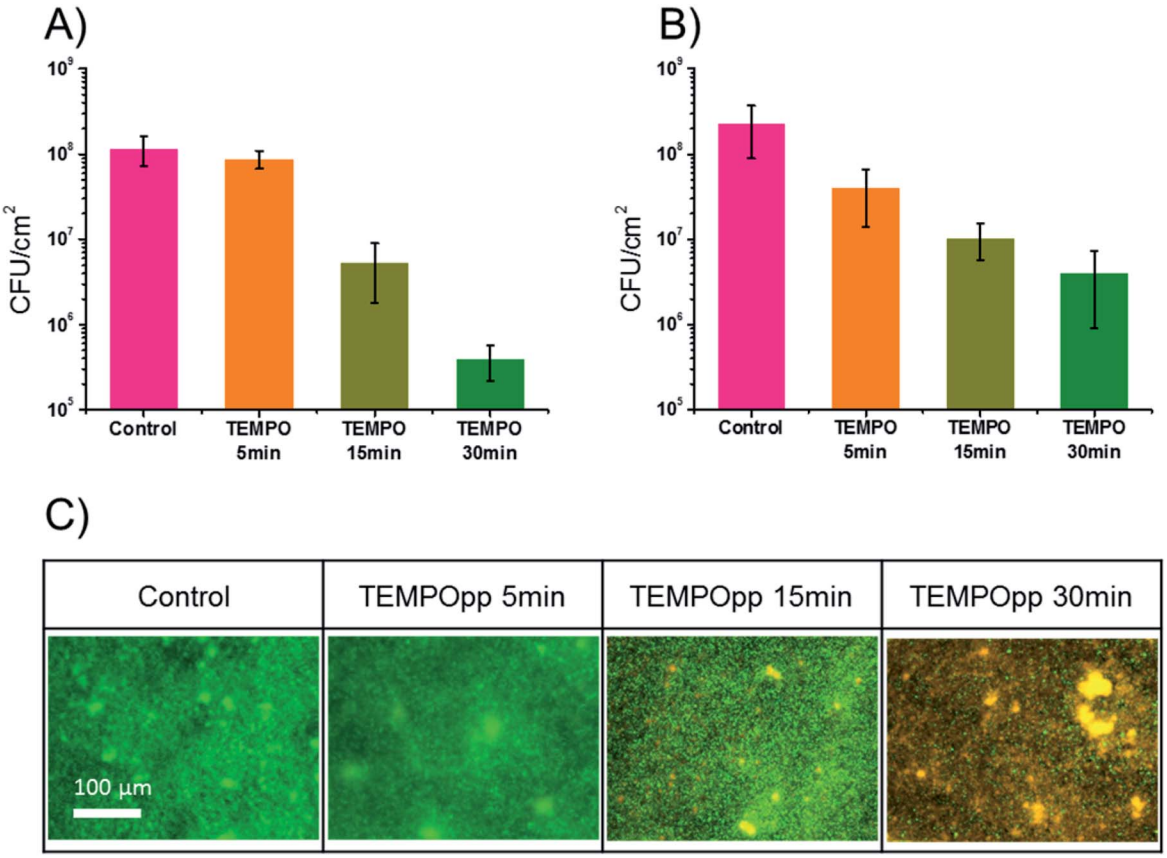

Fig. 2 (A) Quantitative biofilm prevention assay of the TEMPOpp coatings after incubation with *S. epidermidis* for 24 h, $n = 3$, error bars are the respective standard deviation of the population (B) quantitative biofilm dispersion microbiological assay of the TEMPOpp coatings after first growing *S. epidermidis* into a biofilm for 24 h and then contacting the biofilm with the respective coatings for 6 h, $n = 3$, error bars are the respective standard deviation (C) qualitative live/dead images (20×) of the dispersed biofilm.

and less so for those deposited using longer deposition times (TEMPOpp 15 min – 14.8% & TEMPOpp 30 min – 16.2%). As the precursor sublimates rapidly under ambient conditions, these results hint that these coatings contain, in part, oligomeric fragments that volatilize over time. To test this hypothesis, we conducted Electron Paramagnetic Resonance (EPR) measurement of the aqueous supernatant that was in contact with TEMPOpp 30 min overnight (Fig. 1D). As can be seen, water itself does not contain any detectable unpaired electrons, whereas the water that contacted the TEMPOpp exhibits an EPR signal that is characteristic of TEMPO.[44,45] This result strongly suggests that TEMPO-like molecules are mobile within the coatings and migrate upon contact with water into the aqueous phase.

This chimeric behaviour of the coatings, part crosslinked and part mobile, would for most applications be of a substantial disadvantage. However, we considered whether it could be turned into an advantage instead. Because bacterial biofilm is notorious for its ability to prevent xenobiotics from reaching the bacteria imbedded within, only a handful of smaller molecules have been demonstrated capable of penetrating and causing bacterial dispersion; TEMPO is one of them.[7,15,16] Our reasoning was, henceforth, that if the TEMPOpp coatings are releasing oligomeric TEMPO-like molecule fragments, they would not only prevent biofilm formation but also potentially disperse existing biofilm. If true, this would occur in a thickness-dependent manner because the coatings' thickness correlates with the size of the "reservoir" of mobile TEMPO oligomers. This is an aspect which we have not considered in our previous publication where we have qualitatively shown that TEMPOpp coatings prevent biofilm formation of the clinically relevant *S. epidermidis*.[29] To add to these previous findings, we conducted a quantitative biofilm prevention assay for *S. epidermidis*. As can be seen in Fig. 2A, there is a thickness-dependent bacteria reduction on the TEMPOpp surfaces; by up to two log 10 units for the thickest TEMPOpp 30 min. More importantly, we have conducted a test to disperse established *S. epidermidis* biofilm. For this purpose, a biofilm was first grown for 24 h in tryptic soy broth which leads to the stereotypical biofilm as can be seen in Fig. 2C (control). Upon this, the biofilm was contacted with TEMPOpp plasma polymers in a sandwich-assay for 6 hours. After which the samples were both imaged and quantitatively plated out. Fig. 2B depicts the quantitative reduction of bacteria per cm^2 adhering to the surfaces, which again follows a dose–response manner with the thicker TEMPOpp 30 min coatings exerting the most prominent effect with more than a two log 10

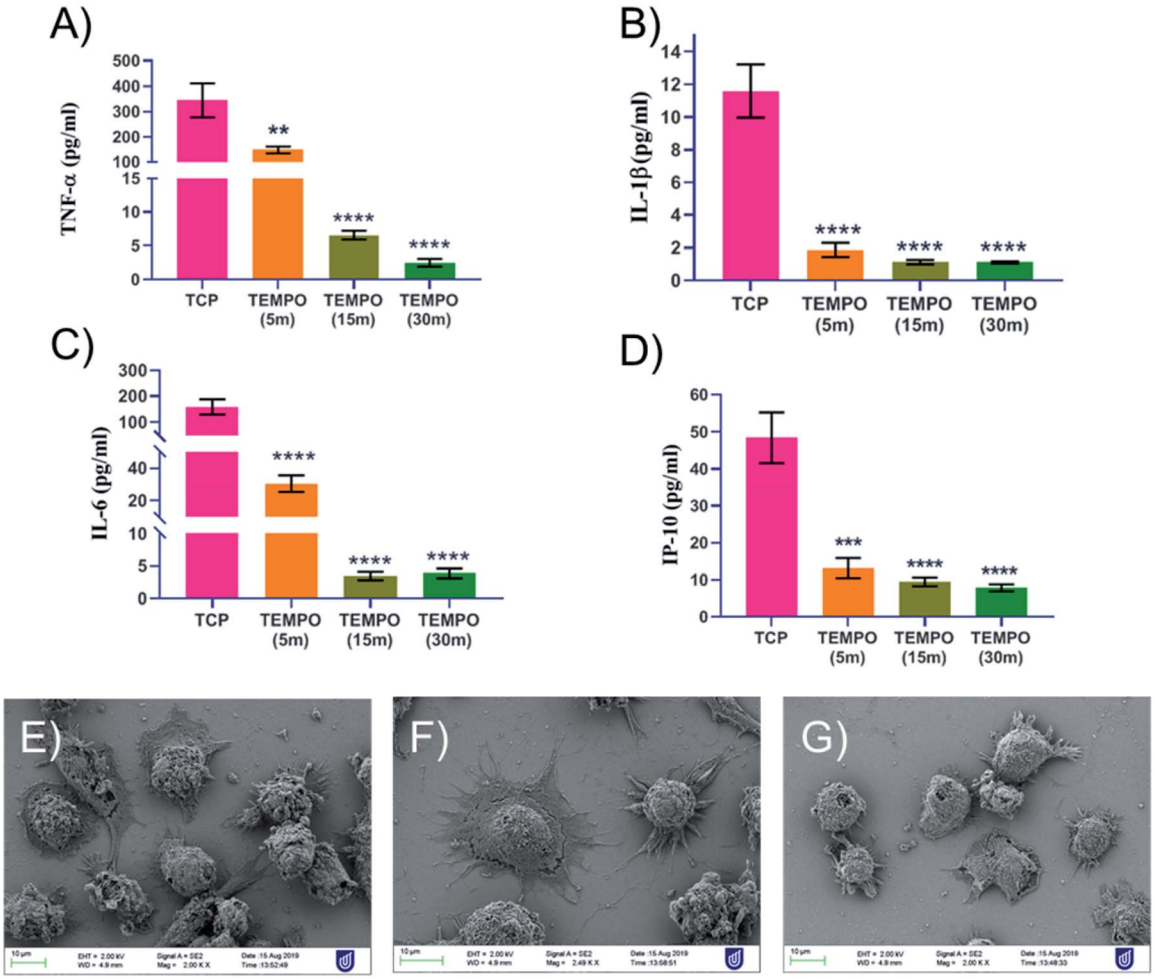

Fig. 3 (A–D) TNF-α, IL-1β, IL-6 and IP-10 cytokine expression of activated THP-1 macrophages upon contacting the surface coatings for 18 h, $n = 3$, statistical significance was determined using a 1-way ANOVA with Dunnett's multiple comparison test (E–G) SEM images of THP-1 macrophages on TEMPOpp 5, 15 and 30 min coatings, respectively.

reduction. The qualitative images can be seen in Fig. 2C where the TEMPOpp 5 min coatings only exert a marginal effect but with increasing thickness of the coatings (TEMPOpp 15 min and TEMPOpp 30 min) the impact of biofilm dispersal becomes increasingly evident. Additional micrographs are found in Fig. S2.† We also conducted a histogram analysis of the live/dead stain which reveals a marked increase in the red optical channel that correlates with the visual results (Fig. S3†). Live/dead staining is a qualitative[46,47] method but, taken together with the quantitative assessment *via* viable CFU colonies, both which we have done, complement each other to paint a thorough picture that the TEMPOpp coatings both prevent and disperse existing biofilm. This result is key for an application which aims to treat chronic wounds.

The second component to help chronic wounds heal is the modulation of uncontrolled inflammation. The inflammation is intertwined with the cytokine expression as well as the macrophage activity, which are both highly elevated in chronic wounds.[48] Thus, regulating cytokine expression is key for better healing outcomes. For example, IL-1β reduction has been correlated with better healing outcomes in human subjects with type 2 diabetes.[49] Similarly, high IL-6 levels were found in wound fluid of chronic wounds, particularly in wounds with a high bacterial load.[50] Analogously, high TNF levels are implicated in many chronic inflammatory conditions.[51] Elevated levels of IP-10 were associated with the dissociation of freshly formed blood vessels with subsequent cell death.[52]

Nitroxide compounds have been shown to modulate the immune response both directly *via* influencing macrophages and indirectly *via* scavenging free RNS and ROS radicals.[53,54] However, detailed work on the cytokine response to nitroxide compounds, such as TEMPO derivatives, is relatively sparse. In contrast, far more work has been done on the physiological messenger nitric oxide (NO).[55] NO, however, has different qualities to the stable nitroxides such as a very short half-life of five seconds and that it may form highly oxidative peroxynitrites. TEMPO derivates, in contrast, do not undergo this process and scavenge the peroxynitrite radicals instead.[56] Peroxynitrites themselves are highly cytotoxic, as researched in work relating to cigarette smoke.[57] Therefore, these critical differences between NO and TEMPO derivatives do not allow for a direct comparison. As for TEMPO derivatives, for example,

their ability to lower IL-6 levels in colon tissue of mice with induced colitis has been demonstrated; attributing the effect to the antioxidative qualities of nitroxides.[58] The same radical-scavenging qualities of nitroxides were put to use in an experiment to demonstrate their protective qualities for fibroblasts against artificially elevated TNF-α levels.[59] The authors attribute this effect not only to the nitroxide scavenging of ROS present but also to the oxidation of ferrous ions, which stops the Fenton reaction;[60] thus stopping the iron-mediated catalysis of hydrogen peroxide to highly cytotoxic hydroxyl radical. Furthermore, TNF-concentration within L929 cells were correlated to spin decay of TEMPO, further indicating an interaction between those two molecules.[61]

Taken all this knowledge together, we challenged activated THP-1 macrophages with our coatings to study their cytokine response (Fig. 3A–D) as well as their adhesion to the coatings themselves (Fig. 3E–G). As can be seen in Fig. 3A–D, the four cytokine factors TNF-α, IL-1β, IL-6 and IP-10 were all down-regulated in a dose-responsive manner correlating with the increasing thickness of the TEMPOpp coatings. The THP-1 cells reacted even more vehemently to the presence of the TEMPOpp coatings than the bacteria, as even TEMPOpp 5 min was capable of inducing a significant reduction of cytokine expression. Analogously, TEMPOpp 15 min & 30 min achieved a highly significant suppression of all four cytokine factors. To study the actual cell interaction with the coatings, we acquired SEM images of the samples (Fig. 3E–G). As can be seen, the activated THP-1 macrophages did form focal adhesion connections, albeit being reluctant to spread out over the surface. Cell lysis was little to none observed with the cells retaining the morphology. Additional SEM images are found in Fig. S4.† Thus, the coatings are modulating the cytokine expression of THP-1 macrophages, while permitting cell adhesion. Taken altogether, the THP-1 results are promising, but it remains a question whether this *in vitro* result would translate into improved healing of chronic wounds *in vivo*. Thus, the next step will be an *in vivo* assay with diabetic mice to evaluate the coatings' efficacy under more complex conditions.

Conclusions

In summary, we have demonstrated that plasma polymerized TEMPO coatings present a new approach to address the two challenges that prevent chronic wounds from healing; namely disperse existing biofilm and modulate cytokine expression. As discussed, the TEMPOpp coatings themselves are a chimeric mixture of cross-linked network with imbrued nitroxide-bearing fragments. The fragments are mobile enough to evaporate with prolonged storage time (4 months) as seen from the loss of thickness over time. This leaching of mobile fragments allows their crossing into the aqueous supernatant, as seen from the EPR measurements. Thus, we used TEMPOpp coatings, with their unique properties, to demonstrate that they are capable of not only preventing biofilm formation but also in dispersing biofilm of *S. epidermidis* in a dose-dependent manner; correlating with the coatings' increasing thickness. This biofilm dispersing effect was evident both from the morphology of the treated biofilm and from the retained number of bacteria on the surfaces. Furthermore, this dose-dependent effect was also evident in significant cytokine reduction of activated THP-1 macrophages which retained their ability to adhere and colonize the surfaces. Thus, in summary, we have exploited the unique qualities of plasma polymerized TEMPO coatings to demonstrate their qualities for treating the two underlying causes of chronic wounds; namely infection and inflammation. Much work remains to explore the full potential of these novel coatings, and we aim to follow up this work with numerous studies; elucidating the coatings and leaching more in detail, study the inflammatory reaction *via* qPCR and flow cytometry, as well as an *in vivo* study using an animal wound model.

Experimental

Chemicals & biological material

TEMPO ((2,2,6,6-tetramethylpiperidin-1-yl)oxyl), tryptic soy broth (TSB), phosphate-buffered saline (PBS), growth agar, Roswell Park Memorial Institute (RPMI) 1460, PMA (phorbol-12-myristate 13-acetate) and THP-1 human cell lines were purchased from Sigma Aldrich and used as received. Silicon wafers 100 mm, CZ, ⟨100⟩, 5–10 ohm, P/boron, 380 ± 25 μm, one side polished, were purchased from MMRC Australia and cut into 1 × 1 cm squares using a disco dicer. Subsequently, these silicon wafers were cleaned using the RCA method.[62] Fetal bovine serum (FBS) and live dead stain were purchased from Thermo Scientific. Penicillin and streptomycin were obtained from Fife Technologies. The LEGENDplex ELISA kits were purchased from BioLegend, San Diego, CA, USA. All kits and solutions were prepared according to the manufacturer's directions and bacterial growth media was autoclaved prior to use.

Plasma polymerization

The general plasma polymerization procedure has been described elsewhere.[63] In short, the 1 × 1 cm silicon wafers were placed into a 13.56 MHz powered plasma reactor and pumped down to base pressure (<10 mTorr). Afterwards, the samples were briefly treated with an air plasma at ~200 mTorr for 1 minute and 50 W to improve adhesion. Afterwards, the samples were pumped down again to base pressure upon which the TEMPO vapours were introduced into the chamber through a ball valve. The pressure was stabilized at 104 mTorr and the plasma was struck at 10 W for either 5, 15 or 30 minutes. Upon finishing, the samples were placed into 24-well plates and stored under ambient conditions.

X-ray photoelectron spectroscopy (XPS)

XPS analysis was done using a Kratos® Axis Ultra DLD spectrometer with a monochromatic Al Kα X-ray source operating at 225 W; the X-ray energy was 1486.6 eV. The analysis area was 0.3 × 0.7 mm. To minimise charging, an internal flood gun was employed. Survey spectra were acquired at a dwell time of 55 ms with 160 eV pass energy, with steps of 0.5 eV using three sweeps.

The data were processed in the CasaXPS software (ver.2.3.16 Casa Software Ltd.®) with Shirley baseline correction.

Scanning electron microscopy (SEM)

The scanning electron microscope used was a (Carl Zeiss Microscopy Merlin with GEMINI II column) operated at 2 kV.

Atomic force microscopy (AFM)

The AFM images were acquired with n NT-MDT NTEGRA SPM AFM. AFM was operated in the noncontact mode with gold-coated silicon nitride tips on the reflective side with resonance frequencies 65–100 kHz. The images were acquired at an amplitude oscillation of 10 nm and with scan rate of 0.5 Hz.

Ellipsometry

The thin films' thicknesses were measured using a J. A. Woollam (Model MC-200) V-Vase ellipsometer with a wavelength range of 400–1000 nm (in 10 nm steps) and alignment angles of 65°, 70° and 75°. The obtained data were fitted with the WVASE32 software (Ver. 3.770) utilizing a two-layer Cauchy mathematical model. By optimizing the optical parameters, the mathematical fit's mean squared error was minimised, thus obtaining the corresponding thickness & deviation.

Electron paramagnetic resonance (EPR)

The EPR spectra were taken using a Magnettech MiniScope MS 5000. 100 μL of MilliQ water was added on TEMPOpp 30 min plasma coating and left for 24 h. The supernatant was subsequently filled into 50 μL ringcaps and inserted into a 3.6 mm quartz EPR tube. The spectra were acquired for a magnetic field of 336 ± 5 mT, a power of 10 mW, a modulation frequency of 100 kHz, an amplitude of 1 × 1000 and sweep time of one minute.

Biofilm prevention

The biofilm assay in question has been used and described previously.[64–66] In short, a −80 °C glycerol stock of *S. epidermidis* ATCC 35984 was streak-plated onto a nutrient agar plate and grown-up overnight at 37 °C. The next day, a single colony was picked from the agar plate and incubated in 20 mL TSB overnight at 37 °C for 24 h. Afterwards, the suspension was diluted to 1.0 McFarland (corresponding to approx. 1×10^8 CFU mL^{-1}) which in turn was further diluted to 1×10^6 CFU mL^{-1} in TSB. The TEMPOpp coated samples and bare silicon wafer (control) were placed into a 24-well plate. Subsequently, 600 μL of the 10^6 CFU mL^{-1} bacterial broth was added to each sample in a 24 well-plate and incubated for 24 h at 37 °C while being agitated at 25 rpm. Subsequently, the samples were washed twice with 600 μL PBS. Afterwards, the samples were placed into 15 mL falcon tubes with 10 mL PBS and sonicated at 30 kHz for 5 minutes and subsequently vortexed for 1 minute. This procedure was done a total of three times per samples to suspend and disperse all bacteria from the surface into the supernatant PBS. The supernatant was subsequently serially diluted in PBS and plated on nutrient agar. A plate count gave the number of viable CFU. The experiments were conducted in triplicates, averaged and the standard deviation used as error bars.

Biofilm dispersion

The biofilm dispersion assay described is an adapted version of a previously published method.[67] It is visualized in Scheme S1† for better understanding. In short, *S. epidermidis* ATCC 35984 was grown up in TSB solution, as described above. Subsequently, this solution was used to grow mature biofilm on bare 1 × 1 cm silicon wafers in 24-well plate by adding 600 μL of 1×10^6 CFU mL^{-1} and incubate these for 24 h at 37 °C and 25 rpm. The resulting biofilm was gently washed twice with 600 μL PBS to remove planktonic bacteria. Afterwards, 100 μL TSB was added onto the biofilm and then sandwiched with the respective TEMPOpp coating. Bare silicon wafers were used as the control. These sandwiched samples were then incubated for 6 h at 37 °C and 25 rpm. Afterwards, the top silicon wafer was gently removed and the samples were rinsed twice with 600 μL PBS. The viable bacterial cell count was done using the same process as for biofilm prevention described above. The experiments were conducted in triplicates, averaged and the standard deviation used as error bars. Separate samples destined for imaging were stained with 50 μL Live/Dead BacLight viability stain (prepared according to the manufacturer's instructions) per silicon wafer and incubated 15 minutes in the dark at room temperature. Subsequently, the samples were then washed twice with 600 μL MilliQ water and imaged with a Nikon Eclipse Ni microscope using a green/red filter and the Nikon digital sight DS-L3 utilizing 490 nm excitation wavelength at 20× magnification. Each sample was micrographed at least 4 times across the whole field of view. For the histogram analysis, three images were split into separate RGB channels, averaged and normalized to an integral of 1 for better comparison; using the FIJI software version 1.52p.

Cell culture & cytokine expression

THP-1 human monocytic cell line was used in this study to assess the inflammatory response. THP-1 cells were cultured in an incubator at 37 °C and 5% CO_2 humidified atmosphere with RPMI 1460 growth medium containing 10% FBS and 1% (v/v) penicillin/streptomycin. THP-1 suspension cells differentiated into adhering macrophages using PMA, THP-1 cells were cultured with media containing 100 ng mL^{-1} PMA for 48 hours and another 24 hours with PMA free media.[68] Differentiated dTHP-1 macrophages were seeded on TEMPO coated glass coverslip with a seeding density of 1×10^5 cells per mL and incubated 18 h for cell attachment. After the overnight cell attachment, growth medium was removed from the culture and cells were washed with PBS and fresh media containing 1 μg mL^{-1} LPS were added to activate the macrophages. After 6 h of incubation conditioned media was collected, and the supernatant was stored in −80 °C for further analysis. Secretion of pro-inflammatory cytokines IL-6, TNF-α, IL-1β and IP-10 were quantified using human LEGENDplex ELISA kits following the manufacturer's instructions. All statistics were performed using graph pad prism 8 software. All data was expressed as mean ±

standard error mean (SEM). Statistical significance was determined using a 1-way ANOVA with Dunnett's multiple comparison test. All experiments were performed thrice in triplicates.

Author contributions

T. D. M.: conceived and designed the analysis & wrote the paper, D. T. T. T.: made samples & collected the data, H. F. K.: contributed data & analysis tools A. Z.: collected the data B. I.: contributed data & analysis tools L. E. G. G.: collected the data R. M. V.: collected the data K. V.: conceived and designed the analysis & wrote the paper.

Conflicts of interest

There are no conflicts to declare.

Acknowledgements

We would like to acknowledge the Australian National Fabrication Facility (ANFF) and Australian Microscopy & Microanalysis Research facility (AMMRF) for the use of their equipment. K. V. thanks NHMRC for fellowship APP1122825 and project grant APP1032738. T. D. M. thanks UniSA for the RTIS Seed Funding.

References

1 T. Bjarnsholt, K. Kirketerp-Møller, P. Ø. Jensen, K. G. Madsen, R. Phipps, K. Krogfelt, N. Høiby and M. Givskov, *Wound Repair Regen.*, 2008, **16**, 2–10.
2 G. Subbiahdoss, R. Kuijer, D. W. Grijpma, H. C. van der Mei and H. J. Busscher, *Acta Biomater.*, 2009, **5**, 1399–1404.
3 L. G. Harris and R. G. Richards, *Injury*, 2006, **37**, S3–S14.
4 F. Gottrup, *Am. J. Surg.*, 2004, **187**, S38–S43.
5 N. Graves and H. Zheng, *Wound Practice & Research*, 2014, **22**(1), 4–12, 14–19.
6 N. A. Richmond, A. D. Maderal and A. C. Vivas, *Dermatol. Ther.*, 2013, **26**, 187–196.
7 D. Fleming and K. P. Rumbaugh, *Microorganisms*, 2017, **5**, 15.
8 A. R. Siddiqui and J. M. Bernstein, *Clin. Dermatol.*, 2010, **28**, 519–526.
9 W.-L. Liu, Y.-L. Jiang, Y.-Q. Wang, Y.-X. Li and Y.-X. Liu, *Chin. Nurs. Res.*, 2017, **4**, 5–8.
10 L. Plate and M. A. Marletta, *Trends Biochem. Sci.*, 2013, **38**, 566–575.
11 C. J. Lowenstein, J. L. Dinerman and S. H. Snyder, *Ann. Intern. Med.*, 1994, **120**, 227–237.
12 G. Schulz and J. Stechmiller, *Int. J. Low. Extrem. Wounds*, 2006, **5**, 6–8.
13 H. Trøstrup, C. J. Lerche, L. Christophersen, P. Ø. Jensen, N. Høiby and C. Moser, *Int. J. Mol. Sci.*, 2017, **18**, 1359.
14 C. Watters, J. A. Everett, C. Haley, A. Clinton and K. P. Rumbaugh, *Infect. Immun.*, 2014, **82**, 92.
15 B. P. Soule, F. Hyodo, K.-i. Matsumoto, N. L. Simone, J. A. Cook, M. C. Krishna and J. B. Mitchell, *Free Radical Biol. Med.*, 2007, **42**, 1632–1650.
16 C. de la Fuente-Núñez, F. Reffuveille, K. E. Fairfull-Smith and R. E. W. Hancock, *Antimicrob. Agents Chemother.*, 2013, **57**, 4877–4881.
17 M. Assayag, S. Goldstein, A. Samuni and N. Berkman, *Free Radic. Biol. Med.*, 2015, **87**, 148–156.
18 M. Lewandowski and K. Gwozdzinski, *Int. J. Mol. Sci.*, 2017, **18**(11), DOI: 10.3390/ijms18112490.
19 A. D. Verderosa, C. de la Fuente-Núñez, S. C. Mansour, J. Cao, T. K. Lu, R. E. W. Hancock and K. E. Fairfull-Smith, *Eur. J. Med. Chem.*, 2017, **138**, 590–601.
20 A. Verderosa, S. Mansour, C. de la Fuente-Núñez, R. Hancock and K. Fairfull-Smith, *Molecules*, 2016, **21**, 841.
21 S.-A. Alexander, C. Kyi and C. H. Schiesser, *Org. Biomol. Chem.*, 2015, **13**, 4751–4759.
22 M. Gozdziewska, G. Cichowicz, K. Markowska, K. Zawada and E. Megiel, *RSC Adv.*, 2015, **5**, 58403–58415.
23 H. Woehlk, M. J. Trimble, S. C. Mansour, D. Pletzer, V. Trouillet, A. Welle, L. Barner, R. E. W. Hancock, C. Barner-Kowollik and K. E. Fairfull-Smith, *Polym. Chem.*, 2019, **10**, 4252–4258.
24 K.-A. Hansen and J. P. Blinco, *Polym. Chem.*, 2018, **9**, 1479–1516.
25 L. J. Martin, B. Akhavan and M. M. M. Bilek, *Nat. Commun.*, 2018, **9**, 357.
26 B. Akhavan, M. Croes, S. G. Wise, C. Zhai, J. Hung, C. Stewart, M. Ionescu, H. Weinans, Y. Gan, S. Amin Yavari and M. M. M. Bilek, *Appl. Mater. Today*, 2019, **16**, 456–473.
27 B. Akhavan, T. D. Michl, C. Giles, K. Ho, L. Martin, O. Sharifahmadian, S. G. Wise, B. R. Coad, N. Kumar, H. J. Griesser and M. M. Bilek, *Appl. Mater. Today*, 2018, **12**, 72–84.
28 M. Macgregor and K. Vasilev, *Materials*, 2019, **12**, 191.
29 T. Michl, J. Barz, C. Giles, M. Haupt, J. H. Henze, J. Mayer, K. Futrega, M. R. Doran, C. Oehr, K. Vasilev, B. R. Coad and H. J. Griesser, *ACS Appl. Nano Mater.*, 2018, **1**(12), 6587–6595.
30 P. Saporito, M. Vang Mouritzen, A. Lobner-Olesen and H. Jenssen, *J. Pept. Sci.*, 2018, **24**, e3080.
31 A. Michelmore, P. Martinek, V. Sah, R. D. Short and K. Vasilev, *Plasma Processes Polym.*, 2011, **8**, 367–372.
32 C. Daunton, L. E. Smith, J. D. Whittle, R. D. Short, D. A. Steele and A. Michelmore, *Plasma Processes Polym.*, 2015, **12**, 817–826.
33 X. Wang, J. Wang, Z. Yang, Y. Leng, H. Sun and N. Huang, *Surf. Coat. Technol.*, 2010, **204**, 3047–3052.
34 J.-C. Ruiz, A. St-Georges-Robillard, C. Thérésy, S. Lerouge and M. R. Wertheimer, *Plasma Processes Polym.*, 2010, **7**, 737–753.
35 T. R. Gengenbach, R. C. Chatelier and H. J. Griesser, *Surf. Interface Anal.*, 1996, **24**, 271–281.
36 A. Choukourov, H. Biederman, D. Slavinska, L. Hanley, A. Grinevich, H. Boldyryeva and A. Mackova, *J. Phys. Chem. B*, 2005, **109**, 23086–23095.
37 G. W. Collins, S. A. Letts, E. M. Fearon, R. L. McEachern and T. P. Bernat, *Phys. Rev. Lett.*, 1994, **73**, 708–711.
38 O. Kylián, A. Choukourov and H. Biederman, *Thin Solid Films*, 2013, **548**, 1–17.

39 R. M. Visalakshan, M. N. MacGregor, A. A. Cavallaro, S. Sasidharan, A. Bachhuka, A. M. Mierczynska-Vasilev, J. D. Hayball and K. Vasilev, *ACS Appl. Nano Mater.*, 2018, **1**, 2796–2807.
40 L. E. Gonzalez Garcia, M. MacGregor-Ramiasa, R. M. Visalakshan and K. Vasilev, *Langmuir*, 2017, **33**, 7322–7331.
41 A. Michelmore, D. A. Steele, J. D. Whittle, J. W. Bradley and R. D. Short, *RSC Adv.*, 2013, **3**, 13540–13557.
42 C. M. Chan, T. M. Ko and H. Hiraoka, *Surf. Sci. Rep.*, 1996, **24**, 1–54.
43 H. J. Griesser and R. C. Chatelier, *J. Appl. Polym. Sci.*, 1990, **46**, 361–384.
44 Y. Sato, H. Hayashi, M. Okazaki, M. Aso, S. Karasawa, S. Ueki, H. Suemune and N. Koga, *Magn. Reson. Chem.*, 2008, **46**, 1055–1058.
45 V. P. Timofeev, A. Y. Misharin and Y. V. Tkachev, *Biophysics*, 2011, **56**, 407.
46 L. Netuschil, T. M. Auschill, A. Sculean and N. B. Arweiler, *BMC Oral Health*, 2014, **14**, 2.
47 M. Berney, F. Hammes, F. Bosshard, H.-U. Weilenmann and T. Egli, *Appl. Environ. Microbiol.*, 2007, **73**, 3283.
48 P. Krzyszczyk, R. Schloss, A. Palmer and F. Berthiaume, *Front. Physiol.*, 2018, **9**, 419.
49 R. E. Mirza, M. M. Fang, W. J. Ennis and T. J. Koh, *Diabetes*, 2013, **62**, 2579–2587.
50 A. Ambrosch, R. Lobmann, A. Pott and J. Preissler, *Int. Wound J.*, 2008, **5**, 99–106.
51 C. Popa, M. G. Netea, P. L. van Riel, J. W. van der Meer and A. F. Stalenhoef, *J. Lipid Res.*, 2007, **48**, 751–762.
52 R. J. Bodnar, C. C. Yates, M. E. Rodgers, X. Du and A. Wells, *J. Cell Sci.*, 2009, **122**, 2064–2077.
53 D. I. Pattison, M. Lam, S. S. Shinde, R. F. Anderson and M. J. Davies, *Free Radic. Biol. Med.*, 2012, **53**, 1664–1674.
54 A. Hosseinzadeh, M. Stylianou, J. P. Lopes, D. C. Müller, A. Häggman, S. Holmberg, C. Grumaz, A. Johansson, K. Sohn, C. Dieterich and C. F. Urban, *Front. Microbiol.*, 2019, **10**(1843), DOI: 10.3389/fmicb.2019.01843.
55 Y. Kobayashi, *J. Leukoc. Biol.*, 2010, **88**, 1157–1162.
56 I. Sadowska-Bartosz and G. Bartosz, *Free Radic. Biol. Med.*, 2015, **86**, S35.
57 I. Rahman, in *Asthma and COPD*, ed. P. J. Barnes, J. M. Drazen, S. I. Rennard and N. C. Thomson, Academic Press, Oxford, 2nd edn, 2009, pp. 293–312, DOI: 10.1016/B978-0-12-374001-4.00025-0.
58 B. Chami, P. T. San Gabriel, S. Kum-Jew, X. Wang, N. Dickerhof, J. M. Dennis and P. K. Witting, *Redox Biol.*, 2020, **28**, 101333.
59 H. Pogrebniak, W. Matthews, J. Mitchell, A. Russo, A. Samuni and H. Pass, *J. Surg. Res.*, 1991, **50**, 469–474.
60 J. B. Mitchell, A. Samuni, M. C. Krishna, W. G. DeGraff, M. S. Ahn, U. Samuni and A. Russo, *Biochemistry*, 1990, **29**, 2802–2807.
61 S. Mishra, *Indian J. Biochem. Biophys.*, 1995, **32**, 254–260.
62 M. Systems, *RCA cleaning procedure*, http://www.microtechprocess.com/pdf/MTS_RCA.pdf.
63 H. J. Griesser, *Vacuum*, 1989, **39**, 485–488.
64 T. D. Michl, B. R. Coad, A. Hüsler, J. D. P. Valentin, K. Vasilev and H. J. Griesser, *Plasma Processes Polym.*, 2016, **13**(6), 654–662.
65 T. D. Michl, B. R. Coad, M. Doran, M. Osiecki, M. H. Kafshgari, N. H. Voelcker, A. Husler, K. Vasilev and H. J. Griesser, *Chem. Commun.*, 2015, **51**, 7058–7060.
66 T. D. Michl, B. R. Coad, M. Doran, A. Husler, J. D. P. Valentin, K. Vasilev and H. J. Griesser, *RSC Adv.*, 2014, **4**, 27604–27606.
67 J. Azeredo, N. F. Azevedo, R. Briandet, N. Cerca, T. Coenye, A. R. Costa, M. Desvaux, G. Di Bonaventura, M. Hebraud, Z. Jaglic, M. Kacaniova, S. Knochel, A. Lourenco, F. Mergulhao, R. L. Meyer, G. Nychas, M. Simoes, O. Tresse and C. Sternberg, *Crit. Rev. Microbiol.*, 2017, **43**, 313–351.
68 R. M. Visalakshan, M. N. MacGregor, S. Sasidharan, A. Ghazaryan, A. M. Mierczynska-Vasilev, S. Morsbach, V. Mailänder, K. Landfester, J. D. Hayball and K. Vasilev, *ACS Appl. Mater. Interfaces*, 2019, **11**(31), 27615–27623.

